

Observation of flat-band localized state in a one-dimensional diamond momentum lattice of ultracold atoms

Chao Zeng(曾超), Yue-Ran Shi(石悦然), Yi-Yi Mao(毛一屹), Fei-Fei Wu(武菲菲), Yan-Jun Xie(谢岩骏), Tao Yuan(苑涛), Han-Ning Dai(戴汉宁), and Yu-Ao Chen(陈宇翱)
Citation: Chin. Phys. B, 2024, 33 (**1**): 010303. DOI: 10.1088/1674-1056/ad0cd1
Journal homepage: http://cpb.iphy.ac.cn; http://iopscience.iop.org/cpb

What follows is a list of articles you may be interested in

Floquet dynamical quantum phase transitions in transverse *XY* spin chains under periodic kickings

Li-Na Luan(栾丽娜), Mei-Yu Zhang(张镁玉), and Lin-Cheng Wang(王林成)
Chin. Phys. B, 2023, 32 (**9**): 090302. DOI: 10.1088/1674-1056/accf68

Wave function collapses and 1/*n* energy spectrum induced by a Coulomb potential in a one-dimensional flat band system

Yi-Cai Zhang(张义财)
Chin. Phys. B, 2022, 31 (**5**): 050311. DOI: 10.1088/1674-1056/ac3653

Superfluid states in α-T_3 lattice

Yu-Rong Wu(吴玉容) and Yi-Cai Zhang(张义财)
Chin. Phys. B, 2021, 30 (**6**): 060306. DOI: 10.1088/1674-1056/abea8a

Collapses-revivals phenomena induced by weak magnetic flux in diamond chain

Na-Na Chang(常娜娜), Wen-Quan Jing(景文泉), Yu Zhang(张钰), Ai-Xia Zhang(张爱霞), Ju-Kui Xue(薛具奎), Su-Peng Kou(寇谡鹏)
Chin. Phys. B, 2020, 29 (**1**): 010306. DOI: 10.1088/1674-1056/ab6087

Topologically protected edge gap solitons of interacting Bosons in one-dimensional superlattices

Xi-Hua Guo(郭西华), Tian-Fu Xu(徐天赋), Cheng-Shi Liu(刘承师)
Chin. Phys. B, 2018, 27 (**6**): 060307. DOI: 10.1088/1674-1056/27/6/060307

RAPID COMMUNICATION

Observation of flat-band localized state in a one-dimensional diamond momentum lattice of ultracold atoms

Chao Zeng(曾超)[1,2,3], Yue-Ran Shi(石悦然)[4,5], Yi-Yi Mao(毛一屹)[1,2,3], Fei-Fei Wu(武菲菲)[1,2,3], Yan-Jun Xie(谢岩骏)[1,2,3], Tao Yuan(苑涛)[1,2,3], Han-Ning Dai(戴汉宁)[1,2,3,†], and Yu-Ao Chen(陈宇翱)[1,2,3]

[1] *Hefei National Research Center for Physical Sciences at the Microscale and School of Physical Sciences, University of Science and Technology of China, Hefei* 230026, *China*

[2] *Shanghai Research Center for Quantum Sciences and CAS Center for Excellence Quantum Information and Quantum Physics, University of Science and Technology of China, Shanghai* 201315, *China*

[3] *Hefei National Laboratory, University of Science and Technology of China, Hefei* 230088, *China*

[4] *Department of Physics, Renmin University of China, Beijing* 100872, *China*

[5] *Key Laboratory of Quantum State Constructuion and Manipulation (Ministry of Education), Renmin University of China, Beijing* 100872, *China*

(Received 6 November 2023; revised manuscript received 13 November 2023; accepted manuscript online 16 November 2023)

We investigated the one-dimensional diamond ladder in the momentum lattice platform. By inducing multiple two- and four-photon Bragg scatterings among specific momentum states, we achieved a flat band system based on the diamond model, precisely controlling the coupling strength and phase between individual lattice sites. Utilizing two lattice sites couplings, we generated a compact localized state associated with the flat band, which remained localized throughout the entire time evolution. We successfully realized the continuous shift of flat bands by adjusting the corresponding nearest neighbor hopping strength, enabling us to observe the complete localization process. This opens avenues for further exploration of more complex properties within flat-band systems, including investigating the robustness of flat-band localized states in disordered flat-band systems and exploring many-body localization in interacting flat-band systems.

Keywords: diamond lattice, flat band, momentum lattice, localized state

PACS: 03.65.Vf, 03.67.Ac, 37.10.Jk **DOI:** 10.1088/1674-1056/ad0cd1

1. Introduction

The exploration of localization properties in disordered systems holds significant importance in realms of solid-state physics and condensed matter physics.[1] Disorder has a significant impact on wave propagation, leading to the well-documented phenomenon of Anderson localization.[2] Even in the presence of interparticle interactions, these localized properties persist, referred to as many-body localization.[3,4] Unconventional localization can also occur in certain disorder-free systems that contain dispersionless or flat bands.[5–7] The eigenstates of flat bands are characterized by perfectly compact localized modes that occupy only a limited number of unit cells. This spatial restriction is due to the lattice geometry, which induces destructive interference among various propagation pathways.[8,9] These highly degenerate flat-band localized states can be lifted by even the weakest disorder. In instances where the flat band intersects other dispersive bands, the system's sensitivity to disorder is markedly heightened. However, in a gapped system, the localized state within the flat band exhibits resilience against weak disorder. The competition between the flat band and disorder in such a gapped system can provoke a transition from flat band localization to Anderson localization (FBL–AL). This transition occurs as the flat band converges with other dispersive bands under the influence of disorder.[10,11] Additionally, an inverse Anderson transition is conceivable in higher dimensions[12] or in specially designed disordered systems.[13] An investigation into the role of the energy gap can significantly deepen our understanding of flat band systems' behavior.

From an experimental perspective, various experimental platforms, such as ultracold quantum gas,[14–16] cavity polaritons[17,18] and photonic crystals,[19–23] have been utilized to study the flat-band systems. Studying the influence of the gap between the flat band and other dispersion bands on the robustness of the flat band system requires precise control of the coupling strength at the single-site level and the capability to measure the time-dependent transport process. These features are often absent in most solid-state systems. Conversely, momentum lattices, where distinct momenta simulate synthetic lattice sites, afford the precise tuning of tunneling strength and phase, as well as the on-site energy of individual sites by manipulating the corresponding laser parameters.[13,24–26] The manipulation includes modifying the frequency, intensity, and phase of a laser, which posits momentum lattices as a versatile platform for studying the more intricate properties of flat-band systems.

In this paper, we report an experimental realization of a highly controllable flat-band system using a Bose–Einstein

†Corresponding author. E-mail: daihan@ustc.edu.cn

© 2024 Chinese Physical Society and IOP Publishing Ltd

condensate (BEC) of ^{87}Rb atoms in a one-dimensional (1D) momentum lattice. Here, we can precisely modulate the inter-site coupling strength, influencing the gap between the flat and dispersive bands. Initially, we engineered a diamond flat-band model comprising 16 sites by adjusting the coupling strengths between the nearest and next-nearest lattice sites. We then prepared the flat-band eigenstate of the diamond lattice system by manipulating the coupling between two lattice sites, confirmed by observing nondiffusive behavior. For comparative analysis, we generated distinct initial states by varying the coupling phase and monitored their entire evolution within the constructed diamond flat-band lattice system. The localization effect was quantified using an 'efficiency' metric. By adjusting specific nearest-neighbor coupling strengths, we achieved the continuous shift of flat bands, thereby modulating the inter-space between the bands and affecting the gap between the flat bands and the dispersive bands. Our work demonstrates the powerful capabilities to dynamically adjust parameters such as the coupling strength and phase between lattice sites. These include assessing the robustness of localized states in disordered flat-band environments and exploring many-body localization within interacting flat-band contexts.

2. Diamond lattice model

Figure 1(a) illustrates the proposed one-dimensional diamond lattice model comprising three distinct sub-lattice sites labelled A, B, and C, characterized by two different hopping strengths, denoted as u and v. The Hamiltonian of an N-site diamond model is expressed as

$$\begin{aligned}\hat{H} = & -v\sum_{i=1}^{N/3}(\hat{c}^{\dagger}_{i,\mathrm{A}}\hat{c}_{i,\mathrm{B}}+\hat{c}^{\dagger}_{i,\mathrm{C}}\hat{c}_{i,\mathrm{B}}+\hat{c}^{\dagger}_{i-1,\mathrm{A}}\hat{c}_{i,\mathrm{B}}+\hat{c}^{\dagger}_{i-1,\mathrm{C}}\hat{c}_{i,\mathrm{B}}+\mathrm{H.c.})\\ & -u(\hat{c}^{\dagger}_{i,\mathrm{A}}\hat{c}_{i,\mathrm{C}}+\mathrm{H.c.})\\ & +\sum_{i=1}^{N/3}(W_{i,\mathrm{A}}\hat{c}^{\dagger}_{i,\mathrm{A}}\hat{c}_{i,\mathrm{A}}+W_{i,\mathrm{B}}\hat{c}^{\dagger}_{i,\mathrm{B}}\hat{c}_{i,\mathrm{B}}+W_{i,\mathrm{C}}\hat{c}^{\dagger}_{i,\mathrm{C}}\hat{c}_{i,\mathrm{C}}),\end{aligned} \tag{1}$$

where $W_{i,\alpha}$ represents the on-site disorder potential, to be discussed in the final section. For the present analysis, we set $W_{i,\alpha}=0$. The single particle dispersion reveals three distinct energy bands

$$E=-u,\ [u\pm\sqrt{u^2+32v^2\cos^2(k)}]/2, \tag{2}$$

as depicted in Fig. 1(b). The flat band, which is located at $E=-u$, is robust against direct coupling u between the A and C sublattices, and is separated from other dispersion bands once $u>2v$. The eigenstate of the flat band only occupies the sub-sites A and C in one unit cell $|\Psi\rangle_i^{\mathrm{FB}}=(\frac{\sqrt{2}}{2}\hat{c}^{\dagger}_{i,\mathrm{A}}-\frac{\sqrt{2}}{2}\hat{c}^{\dagger}_{i,\mathrm{C}})|\mathrm{vac}\rangle$ with $|\mathrm{vac}\rangle$ the vacuum state, as shown in Fig. 1(a) (the two shaded sites).

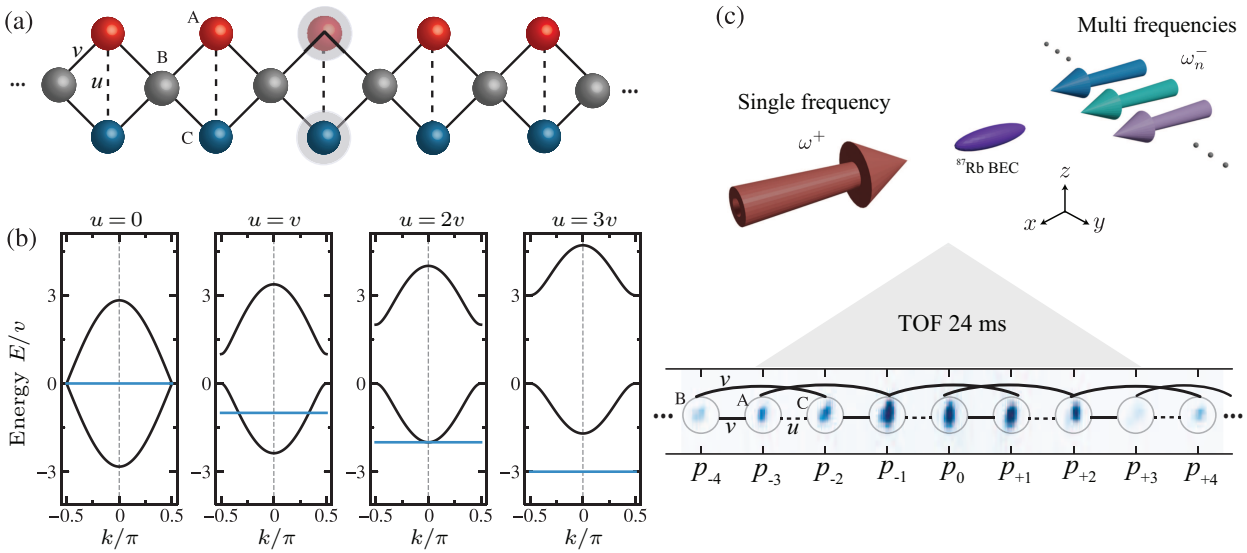


Fig. 1. (a) Schematic diagram of a one-dimensional (1D) diamond model with two kinds of coupling strengths u and v. (b) Band structure of the diamond model with parameters $u=0$, $u=v$, $u=2v$ and $u=3v$. (c) Realization of a 1D momentum lattice using the Bragg process (top) and visualized via time-of-flight imaging (bottom).

3. Experimental preparation

In our experiment configuration, we realized the Hamiltonian describing a diamond lattice (represented by Eq. (1)) in a momentum-space lattice, where the individual momentum states correspond to specific lattice sites. As depicted in Fig. 1(c), our method involved utilizing an optically trapped BEC comprising approximately 6×10^4 ^{87}Rb atoms. The BEC was subjected to the influence of a pair of counter-propagating lasers operating at a wavelength of $\lambda=1064$ nm. One of these lasers maintained a single frequency component, while the other beam encompassed multiple discrete frequency components, meticulously selected to align with various two-photon

and four-photon Bragg resonance conditions. The laser with a constant wavelength cooperated with each individual frequency component of the other beam to establish resonant coupling among a set of momentum states, facilitating coherent transfer and thereby constructing a one-dimensional synthetic lattice.[24,25] These momentum states were associated with discrete momentum values $p_n = 2n\hbar k$, where $k = 2\pi/\lambda$ denotes the laser's wave vector and n signifies the site index. Within this momentum-space lattice framework, we were able to independently regulate the coupling strength, coupling phase, and on-site energy on a site-by-site basis by adjusting the parameters of the lasers. This experimental setup allowed the successful simulation of various one-dimensional lattice models.

To demonstrate the localization effect, it is crucial to initialize the system at an eigenstate of the flat band in the diamond lattice and observe its time evolution. Our process commenced with a BEC initialized in the zero momentum state $|0\rangle$, as illustrated in step (1) of Fig. 2(a). Subsequently, in step (2), a pair of Bragg lasers were employed to induce coupling between states $|0\rangle$ and $|+1\rangle$, facilitating the population of particles into the $|+1\rangle$ states as the system evolves. The final state was determined by the strength α, the phase θ, and the duration time t of the Bragg process. In our experiment, we chose $\alpha \approx 2\pi\hbar \times 2$ kHz and $t \approx 1/16$ ms for the initial state preparations. These chosen parameters were tailored to achieve the desired particle population ratio of 1:1.

In determining the appropriate coupling phase θ, theoretical calculations considering only nearest-neighbor hopping propose setting θ at 0.5π. However, the validity of this theoretical suggestion cannot be confirmed solely by measuring the state population. In fact, the particle fractions would exhibit the same values for all different choices of θ. To determine the correct coupling phase, we followed a method where we initially prepared a state with a specific value of θ. Subsequently, we employed another Bragg process with parameters $\alpha_1 \approx 2\pi\hbar \times 2$ kHz and $\theta = 0$ in the prepared state. Then, we measured the particle occupation on different sites after an evolving time t_1, as depicted in step (3) of Fig. 2(a). In an ideal scenario where the state is perfectly prepared as $|\phi_0\rangle$, it can be demonstrated that the particle fractions for $|0\rangle$ and $|+1\rangle$ should remain constant at a 1:1 ratio throughout the entire evolution process. Specifically, the atomic probability of the $|0\rangle$ momentum state should consistently remain at $P_0 = 0.5$, attributed to the complete destructive interference of hopping to the neighboring site. However, in cases where the state is prepared with errors, P_0 will deviate from 0.5 and display temporal variation.

In Fig. 2(b), we illustrate the results of $P_0(t_1)$ following an evolution of approximately $t_1 \approx 1/16$ ms subsequent to the zero-phase Bragg process. The experimental data (red solid dots) agree well with the numerical simulation (blue solid lines), indicating that $P_0 \approx 0.5$ when the value of θ is approximately around -0.5π and 0.5π.

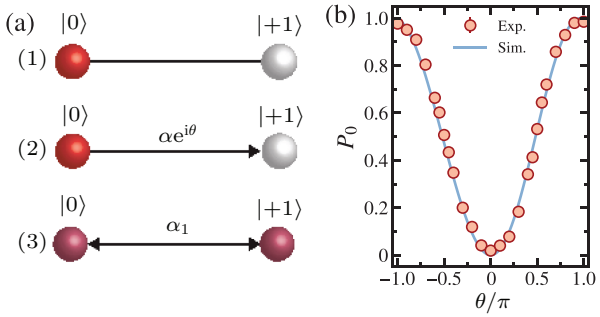


Fig. 2. (a) The initial state preparation process. The BEC is first prepared in the zero momentum state (top), and partially transferred to the $|+1\rangle$ states with a proper phase via Bragg processes (middle). The resulting state is then verified by the evolution of particle occupation (bottom). (b) The population of the zero momentum state as a function of phase θ. The best choice of θ can be optimized by this process.

4. Observation of the localized state

Having prepared an eigenstate of the flat band in a diamond lattice, it is subsequently necessary to experimentally observe the localization effect of its eigenstates in this system. As a comparison, we also prepared other initial states with different θ and observe their localization effect. Experimental measurements, detailed in Fig. 3(a), depict the time evolution of the prepared initial states with phases of 0.5π and -0.5π over a duration of $1.57\hbar/v$. The results of the corresponding numerical simulations are presented in Fig. 3(b). The data illustrate a consistent alignment between experimental observations and numerical simulations throughout the evolution. When $\theta = 0.5\pi$, the localization effect is obvious and the atoms basically stay in the initial two lattice sites with only a small number of atoms diffusing into the high momentum state, while when $\theta = -0.5\pi$, the atoms diffuse rapidly into the high momentum state lattice sites. This result implies that 0.5π is the coupling phase needed to prepare the eigenstate.

To quantify the localization effect, we define the "efficiency" F as described in Ref. [27], in terms of the normalized number of atoms P_n^m of a given state m detected at the lattice site n

$$F_m = \left(\sum_n \sqrt{P_n^{m,\mathrm{diamond}} P_n^{m,\mathrm{expt}}} \right)^2, \tag{3}$$

where the results for a diamond lattice $P_n^{m,\mathrm{diamond}}$ and for the experimental system $P_n^{m,\mathrm{expt}}$ are both used.

The complete time evolution of F for various initial states is illustrated in Fig. 3(c). To explore the behavior of the system, eight distinct coupling phases are employed to create different initial states and observe their evolution within the system. Observing the results, when the phase $\theta = 0.5\pi$ is employed, the prepared initial states manifest the most significant

localization effect, maintaining a consistently localized state throughout the evolution. The observed trend reveals that F predominantly remains above 0.85 during this process, signifying the sustained preservation of the initial state throughout the evolution. This persistence aligns more closely with the characteristics of the eigenstate. On the other hand, when $\theta = -0.5\pi$, the converged value of F drops below 0.4, indicating substantial deviation from the corresponding eigenstate within the diamond model. The remaining six initial states, prepared with other phases, exhibit comparatively lower converged values of F during the evolution compared to the case of $\theta = 0.5\pi$.

We further calculate the time-averaged efficiency $\langle F\rangle_T$ for the states prepared with various θ. Figure 3(d) illustrates our findings. The experimental data for $\theta \approx 0.5\pi$ predominantly exhibit localization and demonstrate significant agreement with the numerical simulations conducted using the time-dependent Hamiltonian. Notably, the maximum value of F reaches approximately 0.88. Based on these compelling results, we establish $\theta \approx 0.5\pi$ as the optimal setting for the preparation of the initial state $|\phi_0\rangle$.

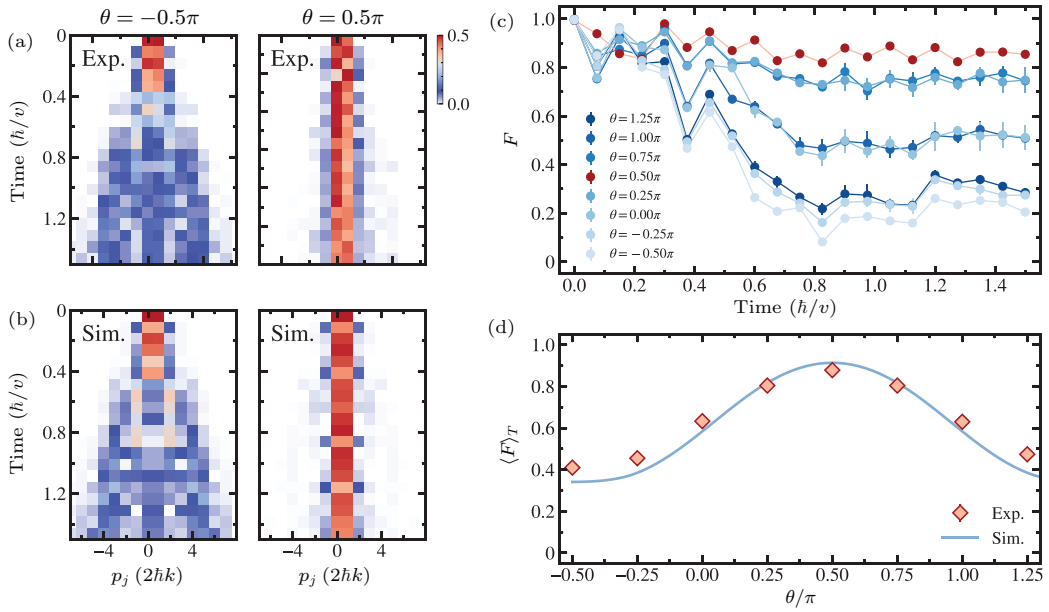


Fig. 3. (a) The particle populations (false color) of different sites upon time evolution are measured for cases of $\theta = -0.5\pi$ and $\theta = 0.5\pi$ when $u = 0$. (b) The same results obtained from numerical simulation. Both panels are taken with $|v| \approx 2\pi\hbar \times 0.25$ kHz in a diamond lattice of 16 sites. (c) Experimental time evolution of the efficiency F for $\theta = -0.5\pi$, -0.25π, 0, 0.25π, 0.5π, 0.75π, π and 1.25π (circles with error bars). (d) The time averaged efficiency $\langle F\rangle_T$ as a function of coupling phase θ. Experimental data (red solid dots with error bars smaller than the size of dots) are averaged over the whole time evolution. The solid blue curve represents a numerical simulation with realistic experimental parameters. The maxima of both the experimental and simulation results are around $\theta \approx 0.5\pi$.

We have thus realized the diamond flat-band system and prepared flat-band eigenstates. According to the structural specifics of the diamond model, we modulated the strengths of certain next-nearest-neighbor couplings u to alter the energy gap between the flat band and the dispersive energy band. This manipulation is represented in Fig. 1(b). Specifically, in the experimental setup, we introduced settings where u equaled v, $2v$, and $3v$ respectively. These adjustments were instrumental in varying the number of intersections between the flat band and the dispersive energy band.

The experimentally observed time evolution of different u values over a duration of $1.57\hbar/v$ is depicted in Fig. 4(a), while the corresponding outcomes from numerical simulations are illustrated in Fig. 4(b). Additionally, the computation of the time-averaged efficiency $\langle F\rangle_T$ for the three distinct situations is presented in Fig. 4(c). The results clearly demonstrate a substantial localization effect for all three localized states. This suggests the successful realization of different localized states within the same model, each exhibiting a distinct energy gap. In our experiment, we exclusively focused on investigating the localization properties of these states without introducing additional localization factors such as disorder or analogous external fields. The observed localization properties strongly suggest the presence of a flat band. It is important that sufficiently strong interactions can lead to a self-trapping phenomenon,[28] showing a distinct localization effect. However, it is crucial to note that the interactions in our experiment were relatively weak, exerting only a minor influence on the evolution dynamics. We may demonstrate flat bands directly through experimental measurements.[29] However, this needs extremely small coupling strengths between certain lattice sites and long detection time. The requirement for high measurement accuracy poses a challenge, given the limitation imposed by the system's decoherence time. Additionally, the potential trap and interactions will have a large impact.

One of the interesting properties of the diamond lattice

model is the ability to achieve complete control over the flat band by manipulating the hopping parameters. Then we can tune the position of the flat band $E = -u$ by changing u/v. Additionally, we can realize an all-bands-flat system by adding a phase to hopping parameters,[13,22,30] where all single-particle eigenstates are spatially compact and the single-particle transport is fully suppressed. For non-interacting cases, particles remain confined within a finite volume of the system, which is called Aharonov–Bohm (AB) caging.[31,32] The existence of disorder would highly affect the properties of the system. When the flat band is separated from other dispersive bands by a gap, the eigenstates of the flat band (compact localized states) are robust against weak disorder, and the system enters the Anderson localization phase once the disorder is larger than the gap. When the band gap vanishes, the system is highly sensitive to the disorder. For the gapless case, arbitrarily small disorder will destroy the FBL state. In contrast, once the system is gapped $|u|/v > 2$, the FBL state is robust against weak disorder $W < u$, and finally enters the AL phase when the disorder is strong enough ($W > u$).

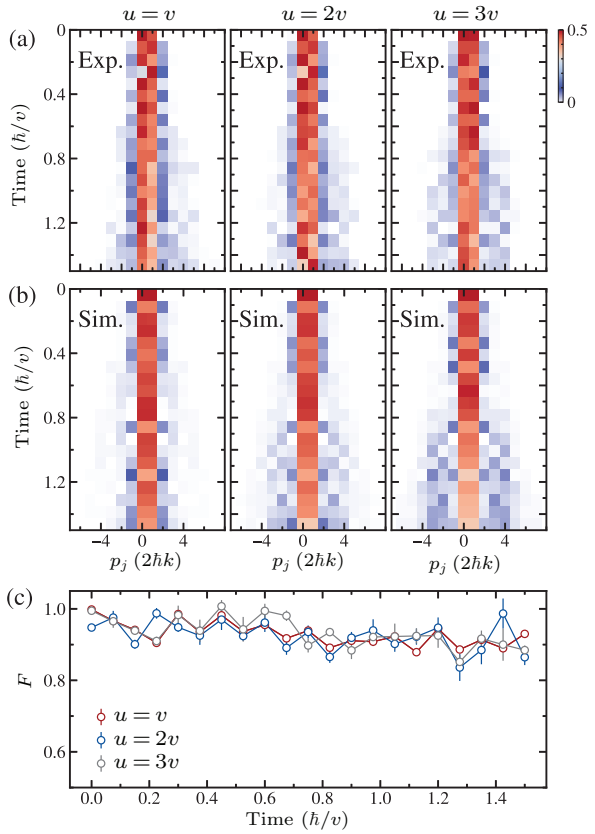


Fig. 4. (a) The particle populations (false color) of different sites upon time evolution are measured for cases of $u = v$, $u = 2v$ and $u = 3v$ when $\theta = 0.5\pi$. (b) The same results obtained from numerical simulation. Both panels are taken with $|v| \approx 2\pi\hbar \times 0.25$ kHz in a diamond lattice of 16 sites. (c) Experimental time evolution of the efficiency F for $u = v$, $u = 2v$ and $u = 3v$ (circles with error bars).

5. Conclusion

We have successfully realized a one-dimensional diamond lattice in a momentum lattice system of ultracold atoms. By fine-tuning the strength and phase of the hopping parameter, we engineered a flat band localized state and observed the localization properties via time-of-flight imaging. Our investigation revealed that the location of the flat band will not influence the eigenstate, where the initially prepared state remains perfectly localized throughout the entire time evolution process. The diamond model we explore exhibits a fascinating characteristic: the flat band can be effectively isolated from other dispersive bands by selectively adjusting the hopping parameters between specific sites. Our protocol can also be carried over to two-dimensions by introducing more laser fields capable of coupling other momentum states, which will be challenging for more condensed spectrum of Bragg frequencies and smaller tunneling rates than those employed in previous 1D studies, the finite momentum spread of the condensate and the phase stabilization. Furthermore, we present additional predictions concerning the localization phase of this system. The flat band localized phase is sensitive to even arbitrarily small disorder strengths in the gapless system. However, in gapped cases, it remains robust against finite disorder strength. Our method suggests promising prospects for exploring other types of flat band systems that may exhibit exotic topological[22,33] and transport properties.[13]

Acknowledgments

Project supported by the National Natural Science Foundation of China (Grant No. 12074367), Anhui Initiative in Quantum Information Technologies, the National Key Research and Development Program of China (Grant No. 2020YFA0309804), Shanghai Municipal Science and Technology Major Project (Grant No. 2019SHZDZX01), the Strategic Priority Research Program of Chinese Academy of Sciences (Grant No. XDB35020200), Innovation Program for Quantum Science and Technology (Grant No. 2021ZD0302002), and New Cornerstone Science Foundation.

References

[1] Lagendijk A, van Tiggelen B and Wiersma D 2009 *Phys. Today* **62** 24
[2] Anderson P W 1958 *Phys. Rev.* **109** 1492
[3] Basko D, Aleiner I and Altshuler B 2006 *Ann. Phys.* **321** 1126
[4] Nandkishore R and Huse D 2015 *Annu. Rev. Conden. Matt. Phys.* **6** 15
[5] Derzhko O and Richter J 2006 *Eur. Phys. J. B* **52** 23
[6] Derzhko O, Richter J, Honecker A, Maksymenko M and Moessner R 2010 *Phys. Rev. B* **81** 014421
[7] Niţă M, Ostahie B and Aldea A 2013 *Phys. Rev. B* **87** 125428
[8] Leykam D, Andreanov A and Flach S 2018 *Adv. Phys. X* **3** 1473052
[9] Leykam D and Flach S 2018 *APL Photonics* **3** 070901
[10] Leykam D, Flach S, Bahat-Treidel O and Desyatnikov A 2013 *Phys. Rev. B* **88** 224203
[11] Leykam D, Bodyfelt J D, Desyatnikov A S and Flach S 2017 *Eur. Phys. J. B* **90** 1
[12] Goda M, Nishino S and Matsuda H 2006 *Phys. Rev. Lett.* **96** 126401
[13] Li H, Dong Z, Longhi S, Liang Q, Xie D and Yan B 2022 *Phys. Rev. Lett.* **129** 220403
[14] Jo G B, Guzman J, Thomas C, Hosur P, Vishwanath A and Stamper-Kurn D 2012 *Phys. Rev. Lett.* **108** 045305

[15] Taie S, Ozawa H, Ichinose T, Nishio T, Nakajima S and Takahashi Y 2015 *Sci. Adv.* **1** e1500854

[16] Luo X and Zhang C 2021 *Phys. Rev. Lett.* **126** 103201

[17] Baboux F, Ge L, Jacqmin T, Biondi M, Galopin E, Lemaître A, Gratiet L L, Sagnes I, Schmidt S, Türeci H E, Amo A and Bloch J 2016 *Phys. Rev. Lett.* **116** 066402

[18] Harder T H, Egorov O A, Beierlein J, Gagel P, Michl J, Emmerling M, Schneider C, Peschel U, Höfling S and Klembt S 2020 *Phys. Rev. B* **102** 121302

[19] Vicencio R A, Cantillano C, Morales-Inostroza L, Real B, Mejía-Cortés C, Weimann S, Szameit A and Molina M I 2015 2015 *Phys. Rev. Lett.* **114** 245503

[20] Mukherjee S, Spracklen A, Choudhury D, Goldman N, Öhberg P, Andersson E and Thomson R R 2015 *Phys. Rev. Lett.* **114** 245504

[21] Mukherjee S and Thomson R R 2015 *Opt. Lett.* **40** 5443

[22] Kremer M, Petrides I, Meyer E, Heinrich M, Zilberberg O and Szameit A 2020 *Nat. Commun.* **11** 907

[23] Xia S, Ramachandran A, Xia S, Li D, Liu X, Tang L, Hu Y, Song D, Xu J, Leykam D, Flach S and Chen Z 2018 *Phys. Rev. Lett.* **121** 263902

[24] Gadway B 2015 *Phys. Rev. A* **92** 043606

[25] An F A, Meier E J and Gadway B 2018 *Phys. Rev. X* **8** 031045

[26] Meier E J, An F A, Dauphin A, Maffei M, Massignan P, Hughes T L and Gadway B 2018 *Science* **362** 929

[27] Meier E J, Ngan K, Sels D and Gadway B 2020 *Phys. Rev. Research* **2** 043201

[28] An F A, Sundar B, Hou J, Luo X, Meier E J, Zhang C, Hazzard K R A and Gadway B 2021 *Phys. Rev. Lett.* **127** 130401

[29] Liang Q, Xie D, Dong Z, Li H, Li H, Gadway B, Yi W and Yan B 2022 *Phys. Rev. Lett.* **129** 070401

[30] Longhi S 2021 *Opt. Lett.* **46** 2872

[31] Aharonov Y and Bohm D 1959 *Phys. Rev.* **115** 485

[32] Vidal J, Mosseri R and Douçot B 1998 *Phys. Rev. Lett.* **81** 5888

[33] Jiao Z, Longhi S, Wang X, Gao J, Zhou W, Wang Y, Fu Y, Wang L, Ren R, Qiao L and Jin X 2021 *Phys. Rev. Lett.* **127** 147401